# Fabrication of Microelectromechanical Devices and Systems; Nanoscale Manufacturing

## CHAPTER 29

- Many of the processes and materials used for manufacturing microelectronic devices are also used for manufacturing micromechanical devices and microelectromechanical systems; this chapter investigates topics in the production of very small mechanical and electromechanical products. The chapter begins with considerations of micromachining and surface machining of mechanical structures from silicon.

- The LIGA process and its variations are then described, along with micromolding, EFAB, and various other techniques for replicating small-scale mechanical devices.

- Solid free-form fabrication processes are sometimes suitable for the production of MEMS and MEMS devices.

- The chapter ends with a discussion of the emerging area of nanoscale manufacturing.

**Typical parts made:** Sensors, actuators, accelerometers, optical switches, ink-jet printing mechanisms, micromirrors, micromachines, and microdevices.

**Alternative methods:** Fine blanking, small scale machining, microforming.

## 29.1 Introduction

The preceding chapter dealt with the manufacture of integrated circuits and products that operate purely on electrical or electronic principles, called **microelectronic devices**. These semiconductor-based devices often have the common characteristic of extreme miniaturization. A large number of devices exist that are mechanical in nature and are of a similar size as microelectronic devices. A **micromechanical device** is a product that is purely mechanical in nature, and has dimensions between a few mm and atomic length scales, such as some very small gears and hinges.

A **microelectromechanical device** is a product that combines mechanical and electrical or electronic elements at these very small length scales. A **microelectromechanical system** (MEMS) is a microelectromechanical device that also incorporates an integrated electrical system into one product. Common examples of

**FIGURE 29.1**    SEM view of a micro mechanical system, the L3G4200DH accelerometer, used in popular smartphones. Sensors such as this accelerometer are perhaps the most common application of MEMS. *Source:* Courtesy of STMicroelectronics, Inc.

micromechanical devices are sensors of all types (Fig. 29.1). Microelectromechanical systems include accelerometers in mobile phones, gyroscopes and global positioning systems (GPS), air-bag sensors in automobiles, and digital micromirror devices. Parts made by **nanoscale manufacturing** generally have dimensions that are between $10^{-6}$ and $10^{-9}$ m, as described in Section 29.5.

Many of the materials and manufacturing methods and systems described in Chapter 28 also apply to the manufacture of microelectromechanical devices and systems. However, microelectronic devices are semiconductor-based, whereas microelectromechanical devices and portions of MEMS do not have this restriction; thus, many more materials and processes are suitable for these applications. Regardless, silicon often is used because several highly advanced and reliable manufacturing processes using silicon have been developed for microelectronic applications. This chapter emphasizes the manufacturing processes that are applicable specifically to microelectromechanical devices and systems, but it should be realized that processes and concepts such as lithography, metallization, etching, coating, and packaging described in Chapter 28 still apply.

MEMS and MEMS devices are rapidly advancing, and new processes or variations on existing processes are continually being developed. A significant leap in the numbers of commercial MEMS devices occurred in the past few years as mobile

phones and tablet computers, integrated accelerometers and gyroscopes into their products. However, it should be recognized that many of the processes described in this chapter have not yet become widespread, but are of interest to researchers and practitioners in MEMS, and hold great potential for future applications.

## 29.2  Micromachining of MEMS Devices

The topics described in the preceding chapter dealt with the manufacture of integrated circuits and products that operate purely on electrical or electronic principles. These processes also are suitable for manufacturing devices that incorporate mechanical elements or features. The following four types of devices can be made through the approach described in Fig. 28.2:

1. **Microelectronic devices** are semiconductor-based devices that often have the common characteristics associated with extreme miniaturization, and use electrical principles in their design.
2. **Micromechanical devices** are products that are purely mechanical in nature and have dimensions between atomic length scales and a few mm; very small gears and hinges are examples.
3. **Microelectromechanical devices** are products that combine mechanical and electrical or electronic elements at very small length scales; most sensors are examples of microelectromechanical devices.
4. **Microelectromechanical systems** are microelectromechanical devices that also incorporate an integrated electrical system in one product. Microelectromechanical systems are rare compared with microelectronic, micromechanical, or microelectromechanical devices, typical examples being air-bag sensors and digital micromirror devices.

The production of features from $\mu$m to mm in size is called *micromachining*. MEMS devices have been constructed from **polycrystalline silicon** (*polysilicon*) and **single-crystal silicon**, because the technologies for integrated-circuit manufacture, described in Chapter 28, are well developed and exploited for these devices; other new processes also have been developed that are compatible with the existing processing steps. The use of anisotropic etching techniques (Section 28.8.1) allows the fabrication of devices with well-defined walls and high aspect ratios; for this reason, some MEMS devices have been fabricated from single-crystal silicon.

One of the difficulties associated with the use of silicon for MEMS devices is the high adhesion encountered between components at small length scales and the associated rapid wear (Section 33.5). Most commercial devices are designed to avoid friction by, for example, using flexing springs instead of bearings. However, this approach complicates designs and makes some MEMS devices not feasible. Consequently, significant research is being conducted to identify materials and lubricants that provide reasonable life and performance, and that would allow sliding on the microscale without excessive wear.

Silicon carbide, diamond, and metals (such as aluminum, tungsten, and nickel) have been investigated as potential MEMS materials; various lubricants also have been investigated. It is known, for example, that surrounding the MEMS device in a silicone oil practically eliminates adhesive wear, but it also limits the performance of the device. Self-assembling layers of polymers also are being investigated, as well as novel and new materials with self-lubricating characteristics. However, the tribology of MEMS devices remains a main technological barrier to any further expansion of their already widespread use.

### 29.2.1    Bulk Micromachining

Until the early 1980s, *bulk micromachining* was the most common method of machining at micrometer scales. This process uses orientation-dependent etches on single-crystal silicon (see Fig. 28.15b), an approach that depends on wet etching (Section 28.8) into a surface and stopping on certain crystal faces, doped regions, and etchable films to form a desired structure. As an example of this process, consider the fabrication of the silicon cantilever shown in Fig. 29.2. Using the masking techniques described in Section 28.7, the process changes a rectangular patch of the *n*-type silicon substrate to *p*-type silicon, through boron doping. Etchants such as potassium hydroxide will not be able to remove heavily boron doped silicon; hence, this patch will not be etched.
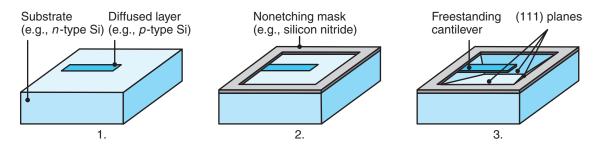
A mask is then produced—for example, with silicon nitride on silicon. When etched with potassium hydroxide, the undoped silicon will be removed rapidly, while the mask and the doped patch will essentially be unaffected. Etching progresses until the (111) planes are exposed in the *n*-type silicon substrate; they undercut the patch, leaving a suspended cantilever (as shown in Fig. 29.2).

### 29.2.2    Surface Micromachining

Although bulk micromachining is useful for producing very simple shapes, it is restricted to single-crystal materials because polycrystalline materials will not wet etch at different rates in different directions. Many MEMS applications require the use of other materials or material combinations; hence, alternatives to bulk micromachining are needed. One such method is *surface micromachining*, the basic steps of which are illustrated for silicon devices in Fig. 29.3.

In surface micromachining, a spacer or sacrificial layer is deposited onto a silicon substrate coated with a thin dielectric layer, called an *isolation*, or *buffer*, *layer*. Phosphosilicate glass deposited by chemical-vapor deposition is the most common material for a spacer layer, because it etches very rapidly in hydrofluoric acid, a property that is useful in step 5. Step 2 in Fig. 29.3 shows the spacer layer after the application of masking and etching. At this stage, a structural thin film is deposited onto the spacer layer; the film can be polysilicon, metal, metal alloy, or a dielectric (step 3 in Fig. 29.3).
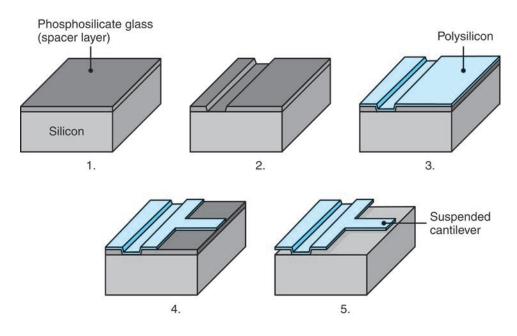
The structural film is then patterned, usually through dry etching, in order to maintain vertical walls and tight dimensional tolerances. Finally, wet etching of the sacrificial layer leaves a freestanding, three-dimensional structure, as shown in step 5 of Fig. 29.3. The wafer must be annealed to remove the residual stresses in the deposited metal before it is patterned, otherwise the structural film will severely warp once the spacer layer is removed.

**FIGURE 29.2**  Schematic illustration of the steps in bulk micromachining. 1. Diffuse dopant in desired pattern. 2. Deposit and pattern-masking film. 3. Orientation-dependent etching (ODE) leaves behind a freestanding structure. *Source:* Courtesy of K.R. Williams.

**FIGURE 29.3**   Schematic illustration of the steps in surface micromachining: 1. Deposition of a phosphosilicate glass (PSG) spacer layer. 2. Lithography and etching of spacer layer. 3. Deposition of polysilicon. 4. Lithography and etching of polysilicon. 5. Selective wet etching of PSG, leaving the silicon substrate and deposited polysilicon unaffected.

Figure 29.4 shows a microlamp that emits a white light when current passes through it; it has been produced through a combination of surface and bulk micromachining. The top patterned layer is a 2.2-$\mu$m layer of plasma-etched tungsten, forming a meandering filament and bond pad. The rectangular overhang is dry-etched silicon nitride. The steeply sloped layer is wet-hydrofluoric acid-etched phosphosilicate glass; the substrate is silicon, which is orientation-dependent etched.

The etchant used to remove the spacer layer must be selected carefully, as it must preferentially dissolve the spacer layer while leaving the dielectric, silicon, and structural film as intact as possible. With large features and narrow spacer layers, this task becomes very difficult, and etching can take many hours. To reduce the etching time, additional etched holes can be designed into the microstructures, to increase access of the etchant to the spacer layer.

Another difficulty that must be overcome is **stiction** after wet etching, which can be described by considering the situation illustrated in Fig. 29.5. After the spacer layer has been removed, the liquid etchant is dried from the wafer 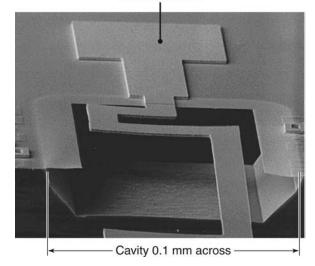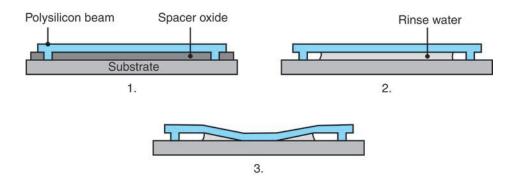surface. A meniscus forms between the layers, resulting in capillary forces that can deform the film and cause contraction of the substrate as the liquid evaporates. Since adhesive forces are more significant at small length scales, it is possible that the film may *stick* permanently to the surface; thus, the desired three-dimensional features will not be produced.



**FIGURE 29.4**   A microlamp produced from a combination of bulk and surface micromachining processes. *Source:* Courtesy of K.R. Williams.

**FIGURE 29.5**   Stiction after wet etching: 1. Unreleased beam. 2. Released beam before drying. 3. Released beam pulled to the surface by capillary forces during drying. Once contact is made, interfacial adhesive forces prevent the beam from returning to its original shape. *Source:* After B. Bhushan.
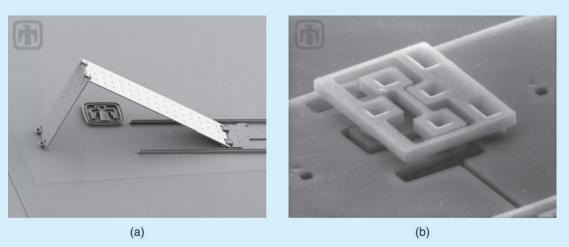
**EXAMPLE 29.1   Surface Micromachining of a Hinge**

Surface micromachining is a widespread technology for the production of MEMS, with applications that include accelerometers, pressure sensors, micropumps, micromotors, actuators, and microscopic locking mechanisms. Often, these devices require very large vertical walls, which cannot be manufactured directly because the high vertical structure is difficult to deposit. This obstacle is overcome by machining large, flat horizontal structures, and then rotating or folding them into an upright position, as shown in Fig. 29.6.
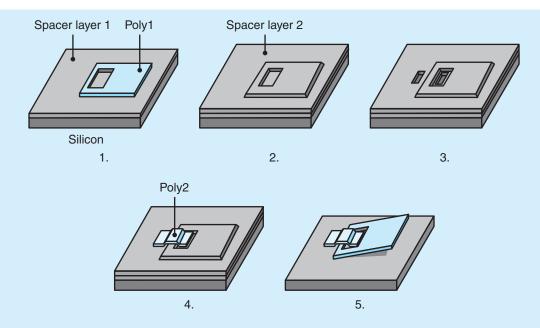
Figure 29.6a shows a micromirror that has been inclined with respect to the surface on which it was manufactured; such systems can be used for reflecting light, that is oblique to a surface, onto detectors or toward other sensors. It is apparent that a device which has such depth, and has the aspect ratio of the deployed mirror, is very difficult to machine directly. Instead, it is easier to surface micromachine the mirror along with a linear actuator, and then to fold the mirror into a deployed position. In order to do so, special hinges (as shown in Fig. 29.6b) are integrated into the design.

Figure 29.7 shows the cross-section of a hinge during its manufacture. The following steps are involved in the production of the hinges:



(a)

(b)

**FIGURE 29.6**   (a) SEM image of a deployed micromirror. (b) Detail of the micromirror hinge. *Source:* Courtesy of Sandia National Laboratories.

**FIGURE 29.7**   Schematic illustration of the steps required to manufacture a hinge. 1. Deposition of a phosphosilicate glass (PSG) spacer layer and polysilicon layer (see Fig. 29.3). 2. Deposition of a second spacer layer. 3. Selective etching of the PSG. 4. Deposition of polysilicon to form a staple for the hinge. 5. After selective wet etching of the PSG, the hinge can rotate.

1. A 2-$\mu$m-thick layer of phosphosilicate glass is first deposited onto the substrate material.
2. A 2-$\mu$m-thick layer of polysilicon (Poly1 in step 1 in Fig. 29.7) is deposited onto the PSG, patterned by photolithography, and dry etched to form the desired structural elements, including the hinge pins.
3. A second layer of sacrificial PSG, with a thickness of 0.5 $\mu$m, is deposited (step 2 in Fig. 29.7).
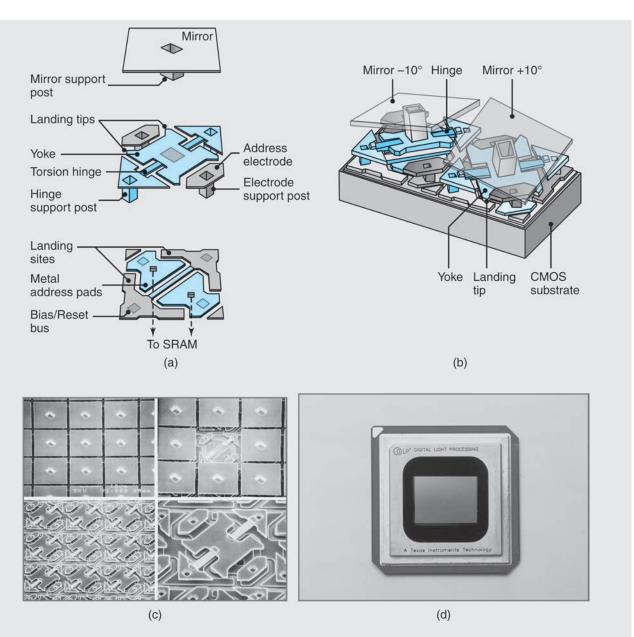4. The connection locations are etched through both layers of PSG (step 3 in Fig. 29.7).

5. A second layer of polysilicon (Poly2 in step 4 in Fig. 29.7) is deposited, patterned, and etched.
6. The sacrificial layers of PSG are then removed by wet etching.

Hinges such as these have very high friction. Thus, if mirrors (as shown in Fig. 29.6) are manipulated manually and carefully with probe needles, they will remain in position. Often, such mirrors will be combined with linear actuators to precisely control their deployment.

## CASE STUDY 29.1   Digital Micromirror Device

An example of a commercial MEMS-based product is the *digital pixel technology* (DPT) device, illustrated in Fig. 29.8. This device uses an array of *digital micromirror devices* (DMD) to project a digital image, as in movie theater projection systems or in nano projectors (Fig. 29.9). The aluminum mirrors can be tilted so that light is directed into or away from the optics that focus light onto a screen. That way, each mirror can represent a pixel of an image's resolution. The mirror allows light or dark pixels to be projected, but levels of gray also can be accommodated. Since the switching time is about 15 $\mu$s (which is much faster than the human eye can respond), the mirror will switch between the on and off states in order to reflect the proper dose of light to the optics.

The fabrication steps for producing the DMD device are shown in Fig. 29.10. This sequence is

(*continued*)

**FIGURE 29.8**   The Texas Instruments digital pixel technology (DPT) device. (a) Exploded view of a single digital micromirror device (DMD). (b) View of two adjacent DMD pixels. (c) Images of DMD arrays with some mirrors removed for clarity; each mirror measures approximately 17 $\mu$m (670 $\mu$in.) on a side. (d) A typical DPT device used for digital projection systems, high-definition televisions, and other image display systems. The device shown contains 1,310,720 micromirrors and measures less than 50 mm (2 in.) per side. *Source:* Courtesy of Texas Instruments.

similar to that of other surface micromachining operations, but has the following important differences:

- All micromachining steps take place at temperatures below 400°C, which is sufficiently low to

ensure that no damage occurs to the electronic circuit.
- A thick silicon-dioxide layer is deposited and is chemical–mechanical polished (Section 26.7) to

**FIGURE 29.9**    A prototype pico projector based on DPT.
*Source:* Courtesy of Texas Instruments Corp.



1. Pattern spacer-1 layer

2. Deposit hinge metal; deposit
   and pattern oxide hinge mask

3. Deposit yoke and pattern
   yoke oxide mask

4. Etch yoke and strip oxide

5. Deposit spacer-2 and mirror

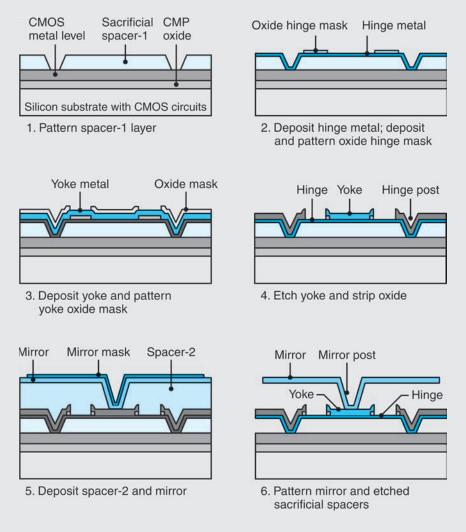6. Pattern mirror and etched
   sacrificial spacers

**FIGURE 29.10**    Manufacturing sequence for the Texas Instruments DMD device.

provide an adequate foundation for the MEMS device.

- The landing pads and electrodes are produced from aluminum, which is deposited by sputtering.
- High reliability requires low stresses and high strength in the torsional hinge, which is produced from a proprietary aluminum alloy.
- The MEMS portion of the DMD is very delicate, and special care must be taken in separating the dies. When completed, a wafer saw (see Fig. 28.6c) cuts a trench along the edges of the DMD, which allows the individual dice to be broken apart at a later stage.
- A special step deposits a layer that prevents adhesion between the yoke and landing pads.

- The DMD is placed in a hermetically sealed ceramic package (Fig. 29.11) with an optical window.

An array of such mirrors represents a grayscale screen. Using three mirrors (one each for red, green, and blue light) for each pixel results in a color image with millions of discrete colors. Digital pixel technology is widely applied in digital projection systems, high-definition television, and other optical equipment. However, to produce the device shown in Fig. 29.8 requires much more than two-and-one-half-dimensional features, thus full three-dimensional, multipart assemblies have to be manufactured.
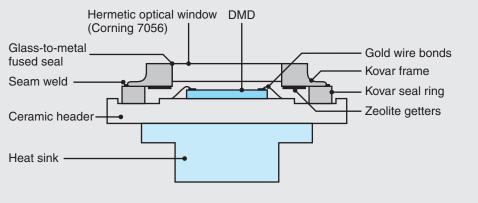


**FIGURE 29.11**   Ceramic flat-package construction used for the DMD device.

**SCREAM.**   Another method for making very deep MEMS structures is the SCREAM (*single-crystal silicon reactive etching and metallization*) process, depicted in Fig. 29.12. In this technique, standard lithography and etching processes produce trenches $10-50$ $\mu$m ($400-2000$ $\mu$in.) deep, which are then protected by a layer of chemically vapor deposited silicon oxide. An anisotropic-etching step removes the oxide only at the bottom of the trench, and the trench is then extended through dry etching. An isotropic etching step (using sulfur hexafluoride, $SF_6$) laterally etches the exposed sidewalls at the bottom of the trench. This undercut (when it overlaps adjacent undercuts) releases the machined structures.

**SIMPLE.**   An alternative to SCREAM is SIMPLE (*silicon micromachining by single-step plasma etching*), as depicted in Fig. 29.13. This technique uses a chlorine-gas-based plasma-etching process that machines $p$-doped or lightly doped silicon anisotropically, but heavily $n$-doped silicon isotropically. A suspended MEMS device can thus be produced in one plasma-etching device, as shown in the figure.

Some of the concerns with the SIMPLE process are:

- The oxide mask is machined, although at a slower rate, by the chlorine-gas plasma; therefore, relatively thick oxide masks are required.
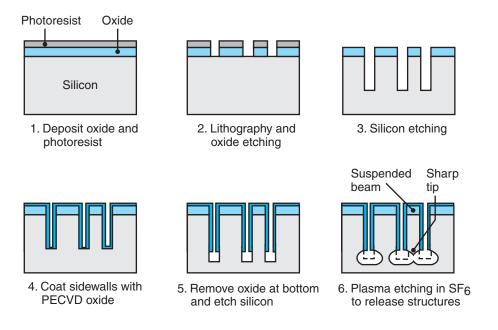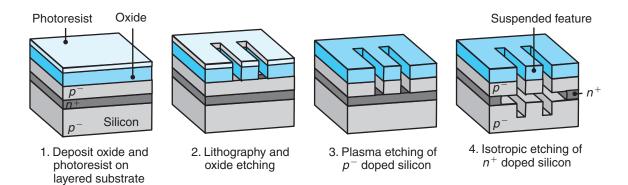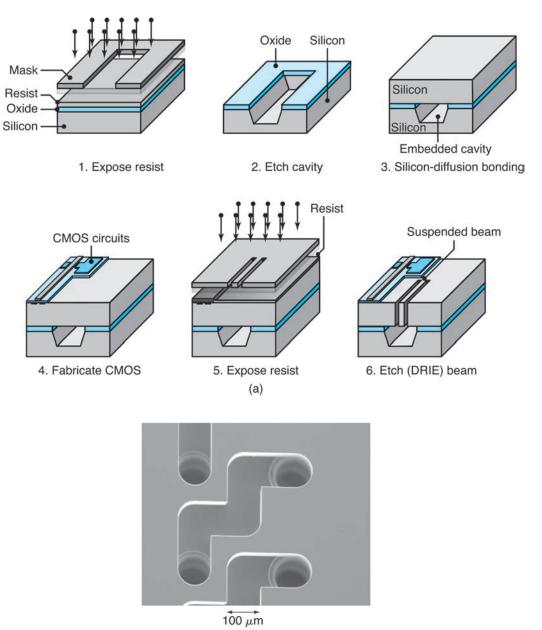
**FIGURE 29.12**  Steps in the SCREAM process. *Source:* After N. Maluf.



**FIGURE 29.13**  Schematic illustration of silicon micromachining by the single-step plasma etching (SIMPLE) process.

- The isotropic etch rate is low, typically 50 nm/min; consequently, this is a very slow process.
- The layer beneath the structures will have developed deep trenches, which may affect the motion of free-hanging structures.

**Etching Combined with Diffusion Bonding.**    Tall structures can be produced in crystalline silicon through a combination of *silicon-diffusion bonding and deep reactive-ion etching* (SFB–DRIE), as illustrated in Fig. 29.14. First, a silicon wafer is prepared with an insulating oxide layer, with the deep trench areas defined by a standard lithography procedure. This step is followed by conventional wet or dry etching to form a large cavity. A second layer of silicon is then fusion bonded to the oxide layer; the second silicon layer can be ground and lapped to the desired

1. Expose resist        2. Etch cavity        3. Silicon-diffusion bonding

4. Fabricate CMOS        5. Expose resist        6. Etch (DRIE) beam

(a)



100 μm

(b)

**FIGURE 29.14**   (a) Schematic illustration of silicon-diffusion bonding combined with deep reactive-ion etching to produce large, suspended cantilevers. (b) A microfluid-flow device manufactured by DRIE etching two separate wafers and then aligning and silicon-fusion bonding them together. Afterward, a Pyrex® layer (not shown) is anodically bonded over the top to provide a window to observe fluid flow. *Source:* (a) After N. Maluf. (b) Courtesy of K.R. Williams.

thickness, if necessary. At this stage, integrated circuitry is manufactured through the steps outlined in Fig. 28.2. A protective resist is applied and exposed, and the desired trenches are then etched by deep reactive-ion etching to the cavity in the first layer of silicon.

**EXAMPLE 29.2    Operation and Fabrication Sequence for a Thermal Ink-jet Printer**
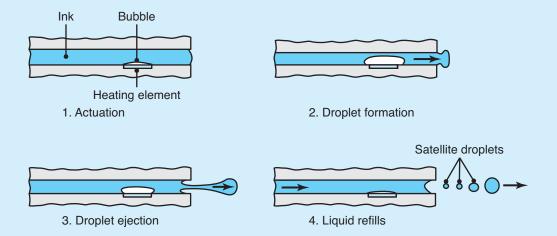
Thermal ink-jet printers are among the most successful applications of MEMS to date. These printers operate by ejecting nano- or picoliters ($10^{-12}$ l) of ink from a nozzle toward the paper. Ink-jet printers use a variety of designs, but silicon-machining technology is most applicable to high-resolution printers. Note that a resolution of 1200 dpi requires a nozzle spacing of approximately 20 $\mu$m.

The mode of operation of an ink-jet printer is shown in Fig. 29.15. When an ink droplet is to be generated and expelled, a tantalum resistor (placed below a nozzle) is heated, which makes a thin film of ink form a bubble within 5 $\mu$s, with internal pressures reaching 1.4 MPa (200 psi). The bubble then expands rapidly, and as a result, the fluid is forced rapidly out of the nozzle. Within 24 $\mu$s, the tail of the ink-jet droplet separates because of surface tension, the heat source is turned off, and the bubble collapses inside the nozzle. Within 50 $\mu$s, sufficient ink has been drawn into the nozzle from a reservoir to form the desired meniscus for the next droplet.
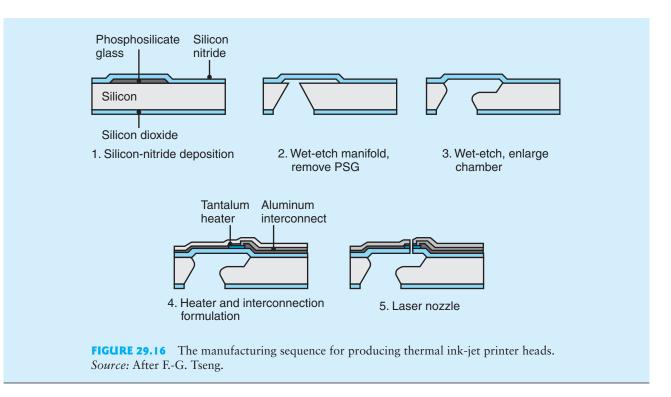
Traditional ink-jet printer heads have been made with electroformed nickel nozzles, produced separately from the integrated circuitry, thus requiring a bonding operation to attach these two components. With increasing printer resolution, it is more difficult to bond the components with a tolerance of less than a few micrometers. For this reason, single-component, or monolithic, fabrication is of interest.

The fabrication sequence for a monolithic ink-jet printer head is shown in Fig. 29.16. A silicon wafer is first prepared and coated with a phosphosilicate-glass (PSG) pattern and a low-stress silicon-nitride coating. The ink reservoir is obtained by isotropically etching the back side of the wafer, followed by PSG removal and enlargement of the reservoir. The required CMOS (complementary metal-oxide semiconductor) controlling circuitry is then produced, and a tantalum heater pad is deposited. The aluminum interconnection between the tantalum pad and the CMOS circuit is formed, and the nozzle is produced through laser ablation. An array of such nozzles can be placed inside an ink-jet printing head, and resolutions of 2400 dpi or higher can be achieved.



**FIGURE 29.15**    Sequence of operation of a thermal ink-jet printer. 1. Resistive heating element is turned on, rapidly vaporizing ink and forming a bubble. 2. Within 5 $\mu$s, the bubble has expanded and displaced liquid ink from the nozzle. 3. Surface tension breaks the ink stream into a bubble, which is discharged at high velocity; the heating element is turned off at this time, so that the bubble collapses as heat is transferred to the surrounding ink. 4. Within 24 $\mu$s an ink droplet (and some undesirable satellite droplets) are ejected, and surface tension of the ink draws more liquid from the reservoir. *Source:* After F.-G. Tseng.

**FIGURE 29.16** The manufacturing sequence for producing thermal ink-jet printer heads.
*Source:* After F.-G. Tseng.

## 29.3 Electroforming-based Processes

### 29.3.1 LIGA

*LIGA* is a German acronym for the combined processes of X-ray lithography, electro-deposition, and molding (in German, X-ray *li*thographie, *g*alvanoformung, und *a*bformung). A schematic illustration of this process is given in Fig. 29.17.
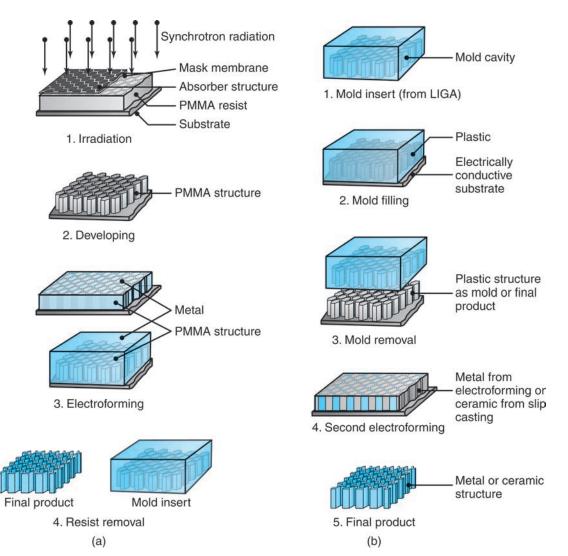
The LIGA process involves the following steps:

1. A relatively thick (up to hundreds of micrometers) resist layer of polymethyl-methacrylate (PMMA) is deposited onto a primary substrate.
2. The PMMA is exposed to columnated X-rays and is developed.
3. Metal is electrodeposited onto the primary substrate.
4. The PMMA is removed or stripped, resulting in a freestanding metal structure.
5. Plastic is injection-molded into the metal structure.

Depending on the application, the final product from a LIGA process may consist of one of the following:

- A freestanding metal structure, resulting from the electrodeposition process
- A plastic injection-molded structure
- An investment-cast metal part, using the injection-molded structure as a blank
- A slip-cast ceramic part, produced using the injection-molded parts as the molds

The substrate used in LIGA is a conductor or a conductor-coated insulator. Examples of primary substrate materials include austenitic steel plate, silicon wafers with a titanium layer, and copper plated with gold, titanium, or nickel. Metal-plated

**FIGURE 29.17** The LIGA (lithography, electrodeposition, and molding) technique. (a) Primary production of a metal final product or mold insert. (b) Use of the primary part for secondary operations or replication. *Source:* Based on data from IMM Institut für Mikrotechnik, Mainz, Germany.

ceramic and glass also have been used. The surface may be roughened by grit blasting to encourage good adhesion of the resist material.

Resist materials must have high X-ray sensitivity, dry- and wet-etching resistance when unexposed, and thermal stability. The most common resist material is polymethylmethacrylate, which has a very high molecular weight (more than $10^6$ per mole; Section 7.2). The X-rays break the chemical bonds, leading to the production of free radicals and to a significantly reduced molecular weight in the exposed region. Organic solvents then preferentially dissolve the exposed PMMA in a wet-etching process. After development, the remaining three-dimensional structure is rinsed and dried, or it is spun and blasted with dry nitrogen.

Two newer forms of LIGA are **UV-LIGA** and **Silicon-LIGA**. In *UV-LIGA*, special photoresists are used, instead of PMMA, and they are exposed through
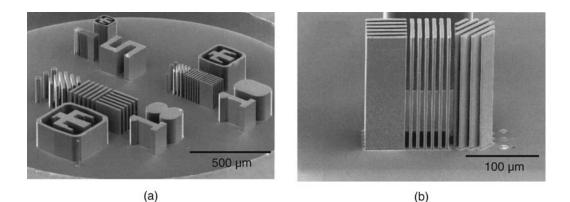
ultraviolet lithography (Section 28.7). *Silicon-LIGA* uses deep reactive-ion-etched silicon (Section 28.8.2) as a preform for further operations. These processes, like the traditional X-ray-based LIGA, are used to replicate MEMS devices, but, unlike LIGA, they do not require the expensive columnated X-ray source for developing their patterns.
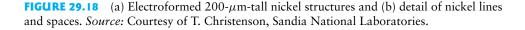
The electrodeposition of metal usually involves the electroplating of nickel (Section 34.9). The nickel is deposited onto exposed areas of the substrate; it fills the PMMA structure and can even coat the resist (Fig. 29.17a). Nickel is the preferred material because of the relative ease in electroplating with well-controlled deposition rates. Electroless plating of nickel also is possible, and the nickel can be deposited directly onto electrically insulating substrates. However, because nickel displays high wear rates in MEMS, significant research is being directed toward the use of other materials or coatings.

After the metal structure has been deposited, precision grinding removes either the substrate material or a layer of the deposited nickel. The process is referred to as *planarization* (Section 28.10). The need for planarization is obvious when it is recognized that three-dimensional MEMS devices require micrometer tolerances, on layers many hundreds of micrometers thick. Planarization is difficult to achieve, because conventional lapping leads to preferential removal of the soft PMMA and smearing of the metal. Planarization usually is accomplished with a diamond-lapping procedure (Section 26.7) referred to as *nanogrinding*. Here, a diamond-slurry-loaded, soft metal plate is used to remove material in order to maintain flatness within 1 $\mu$m (40 $\mu$in.) over a 75-mm (3-in.) diameter substrate.

If cross-linked, the PMMA resist is then exposed to synchrotron X-ray radiation, and removed by exposure to an oxygen plasma or through solvent extraction. The result is a metal structure, which may be processed further. Examples of freestanding metal structures produced through the electrodeposition of nickel are shown in Fig. 29.18.

The processing steps used to make freestanding metal structures are time consuming and expensive. The main advantage of LIGA is that these structures serve as molds for the rapid replication of submicron features through molding operations. The processes that can be used for producing micromolds are shown and compared in Table 29.1, where it can be seen that LIGA provides some clear advantages. Reaction injection molding, injection molding, and compression molding (described in Chapter 19) also have been used to make the micromolds.



(a)                                              (b)

**FIGURE 29.18**   (a) Electroformed 200-$\mu$m-tall nickel structures and (b) detail of nickel lines and spaces. *Source:* Courtesy of T. Christenson, Sandia National Laboratories.

**TABLE 29.1**

| Comparison of Micromold Manufacturing Techniques | | | |
|---|---|---|---|
| | **Production technique** | | |
| Characteristic | LIGA | Laser machining | EDM |
| Aspect ratio | 10–50 | 10 | up to 100 |
| Surface roughness | <50 nm | 100 nm | $0.3-1\mu m$ |
| Accuracy | <1 $\mu m$ | $1-3\mu m$ | $1-5\mu m$ |
| Mask required | Yes | No | No |
| Maximum height | $1-500\mu m$ | $200-500\mu m$ | $\mu m$ to mm |

*Source:* After L. Weber, W. Ehrfeld, H. Freimuth, M. Lacher, M. Lehr, P. Pech, and K.R. Williams.

---

**EXAMPLE 29.3    Production of Rare-earth Magnets**

A number of scaling issues in electromagnetic devices indicate that there is an advantage in using rare-earth magnets from the samarium cobalt (SmCo) and neodymium iron boron (NdFeB) families, which are available in powder form. These alloys are of interest because they can produce magnets that are one order of magnitude more powerful than conventional magnets (Table 29.2). Such materials can be used when effective miniature electromagnetic transducers are to be produced.

The processing steps involved in manufacturing these magnets are shown in Fig. 29.19. The PMMA mold is produced by exposure to X-ray radiation and solvent extraction. The rare-earth powders are mixed with a binder of epoxy and applied to

**TABLE 29.2**

| Comparison of Properties of Permanent-magnet Materials | |
|---|---|
| Material | Energy product (Gauss–Oersted $\times 10^{-6}$) |
| Carbon steel | 0.20 |
| 36% Cobalt steel | 0.65 |
| Alnico I | 1.4 |
| Vicalloy I | 1.0 |
| Platinum–cobalt | 6.5 |
| $Nd_2Fe_{14}B$, fully dense | 40 |
| $Nd_2Fe_{14}B$, bonded | 9 |

*Source:* Courtesy of T. Christenson, Sandia National Laboratories.
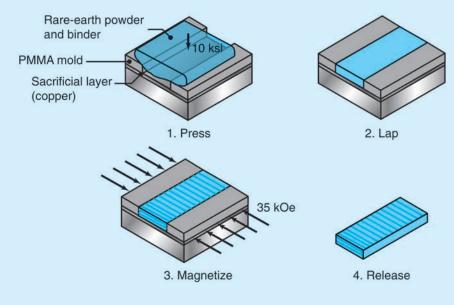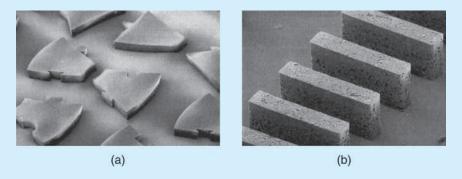


**FIGURE 29.19** Fabrication process used to produce rare-earth magnets for microsensors. *Source:* Courtesy of T. Christenson, Sandia National Laboratories.

the mold through a combination of calendering (see Fig. 19.22) and pressing. After curing in a press at a pressure around 70 MPa (10 ksi), the substrate is planarized. The substrate is then subjected to a magnetizing field, of at least 35 kilo-oersteds (kOe), in the desired orientation. Once the material has been magnetized, the PMMA substrate is dissolved, leaving behind the rare-earth magnets, as shown in Fig. 29.20.



(a)                                   (b)

**FIGURE 29.20**   SEM images of $Nd_2Fe_{14}B$ permanent magnets. The powder particle size ranges from 1 to 5 $\mu$m, and the binder is a methylene-chloride-resistant epoxy. Mild distortion is present in the image due to magnetic perturbation of the imaging electrons. Maximum energy products of 9 MGOe have been obtained with this process. *Source:* Courtesy of T. Christenson, Sandia National Laboratories.

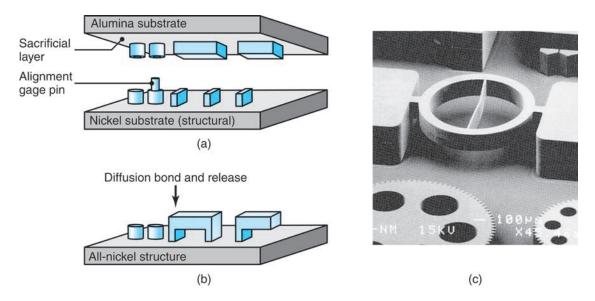### 29.3.2   Multilayer X-Ray Lithography

The LIGA technique is very powerful for producing MEMS devices with large aspect ratios and reproducible shapes. It is, however, often useful to obtain a multilayer stepped structure that cannot be made directly through LIGA. For nonoverhanging part geometries, direct plating can be applied. In this technique, a layer of electrodeposited metal with surrounding PMMA is produced, as previously described. A second layer of PMMA resist is then bonded to this structure and X-ray exposed, using an aligned X-ray mask.

Often, it is useful to have overhanging geometries within complex MEMS devices. A batch diffusion-bonding and release procedure has been developed for this purpose, as schematically illustrated in Fig. 29.21a. This process involves the preparation of two PMMA patterned and electroformed layers, with the PMMA subsequently removed. The wafers are then aligned, face to face, with guide pins that press-fit into complementary structures on the opposite surface. Finally, the substrates are joined in a hot press, and a sacrificial layer on one substrate is etched away, leaving behind one layer bonded to the other. An example of such a structure is shown in Fig. 29.21b.

### 29.3.3   HEXSIL

This process, illustrated in Fig. 29.21, combines *hex*agonal honeycomb structures, *sil*icon micromachining, and thin-film deposition to produce high-aspect-ratio, freestanding structures. HEXSIL can produce tall structures, with a shape definition that rivals that of structures produced by LIGA.

In HEXSIL, a deep trench is first produced in single-crystal silicon by dry etching, followed by shallow wet etching to make the trench walls smoother. The depth

**FIGURE 29.21**    Multilevel MEMS fabrication through wafer-scale diffusion bonding. (a) Two wafers are aligned and assembled. (b) Resultant structure after diffusion bonding and removal of alumina substrate. (c) A suspended ring structure for measurement of tensile strain, formed by two-layer wafer-scale diffusion bonding. *Source:* (c) Courtesy of T. Christenson, Sandia National Laboratories.
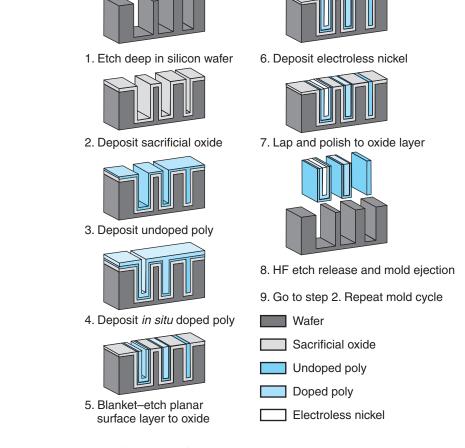
of the trench matches the desired structure height, and is limited practically to around 100 $\mu$m. An oxide layer is then grown or deposited onto the silicon, followed by an undoped-polycrystalline silicon layer, which results in good mold filling and shape definition. A doped-silicon layer then follows, providing a resistive portion of the microdevice. Electroplated or electroless nickel plating is then deposited. Figure 29.22 shows various trench widths to demonstrate the different structures that can be produced in HEXSIL.
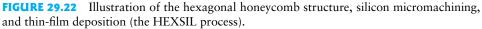
Microscale tweezers produced through the HEXSIL process are shown in Fig. 29.23. A thermally activated bar activates the tweezers, which have been used for microassembly and microsurgery applications.
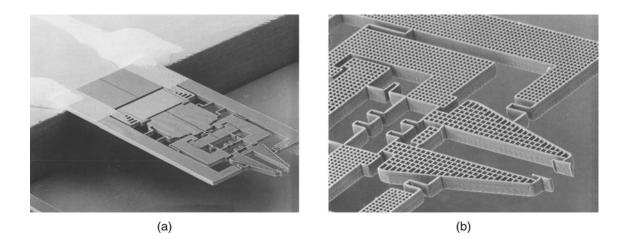
### 29.3.4    MolTun

This process (short for *mol*ding of *tun*gsten) was developed in order to utilize the higher mass of tungsten in micromechanical devices and systems. In MolTun, a sacrificial oxide is patterned through lithography and then etched, but instead of electroforming, a layer of tungsten is deposited through chemical vapor deposition. Excess tungsten is then removed by chemical−mechanical polishing, which also ensures good control over layer thickness. Multiple layers of tungsten can be deposited to develop intricate geometries (Fig. 29.24).

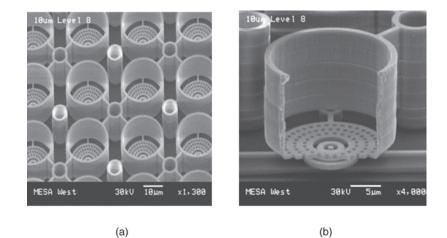MolTun has been used for micro mass-analysis systems and a large number of micro-scale latching relays, which take advantage of tungsten's higher strength compared to other typical MEMS materials. The depth of MolTun structures can be significantly larger than those produced through silicon micromachining; the mass analysis array in Fig. 29.24, for example, has a total thickness of around 25 $\mu$m.

1. Etch deep in silicon wafer

2. Deposit sacrificial oxide

3. Deposit undoped poly

4. Deposit *in situ* doped poly

5. Blanket–etch planar
   surface layer to oxide

6. Deposit electroless nickel

7. Lap and polish to oxide layer

8. HF etch release and mold ejection

9. Go to step 2. Repeat mold cycle

- Wafer
- Sacrificial oxide
- Undoped poly
- Doped poly
- Electroless nickel

**FIGURE 29.22**   Illustration of the hexagonal honeycomb structure, silicon micromachining, and thin-film deposition (the HEXSIL process).

(a)

(b)

**FIGURE 29.23**   (a) SEM image of microscale tweezers used in microassembly and microsurgery applications. (b) Detailed view of gripper. *Source:* Courtesy of MEMS Precision Instruments.

(a)

(b)

**FIGURE 29.24**   An array of micro-mass analysis systems consisting of cylindrical ion traps, constructed of 14 layers of molded tungsten, including 8 layers for the ring electrode. *Source: Courtesy of Sandia National Laboratories.*

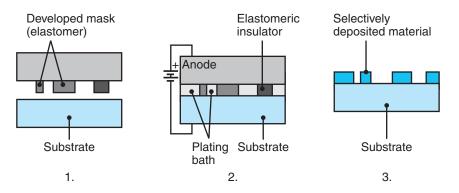## 29.4   Solid Free-form Fabrication of Devices

*Solid free-form fabrication* is another term for *rapid prototyping*, as described in Chapter 20. This method is unique in that complex three-dimensional structures are produced through additive manufacturing, as opposed to material removal. Many of the advances in rapid prototyping also are applicable to MEMS manufacture for processes with sufficiently high resolution. *Stereolithography* (Section 20.3.2) involves curing a liquid thermosetting polymer, using a photoinitiator and a highly focused light source. Conventional stereolithography uses layers between 75 and 500 $\mu$m in thickness, with a laser dot focused to a diameter of 0.05–0.25 mm.

**Microstereolithography.**   *Microstereolithography* uses the same basic approach as stereolithography; however, there are some important differences between the two processes, including the following:

- The laser is more highly focused, to a diameter as small as 1 $\mu$m, as compared with 10 to over 100 $\mu$m in stereolithography.
- Layer thicknesses are around 10 $\mu$m, which is an order of magnitude smaller than in stereolithography.
- The photopolymers used must have much lower viscosities, to ensure the formation of uniform layers.
- Support structures are not required in microstereolithography, since the smaller structures can be supported by the fluid.
- Parts with significant metal or ceramic content can be produced, by suspending nanoparticles in the liquid photopolymer.

The microstereolithography technique has several cost advantages, but the MEMS devices made by this method are difficult to integrate with the controlling circuitry.

**Electrochemical Fabrication.**   The solid free-form fabrication of MEMS devices using instant masking is known as *electrochemical fabrication* (EFAB). Instant masking is one EFAB technique for producing MEMS devices (Fig. 29.25). A mask of

**FIGURE 29.25**   The instant-masking process: 1. Bare substrate. 2. During deposition, with the substrate and instant mask in contact. 3. The resulting pattern deposited. *Source:* Courtesy of Microfabrica.
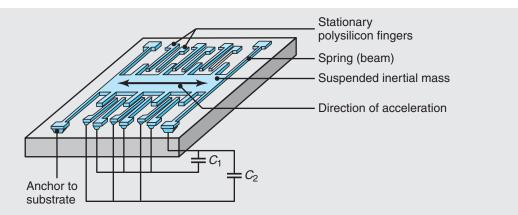
elastomeric material is first produced through conventional photolithography techniques, described in Section 28.7. The mask is pressed against the substrate in an electrodeposition bath, so that the elastomer conforms to the substrate and excludes the plating solution in contact areas. Electrodeposition takes place in areas that are not masked, eventually producing a mirror image of the mask. By using a sacrificial filler, made of a second material, instant masking technology can produce complex three-dimensional shapes complete with overhangs, arches, and other features.

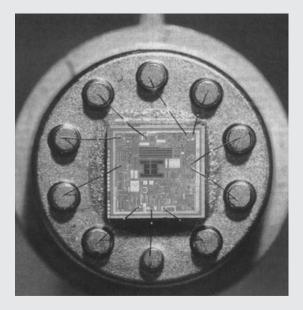## CASE STUDY 29.2   Accelerometer for Automotive Air Bags

Accelerometers based on lateral resonators represent the largest commercial application of surface micromachining today, and are used widely as sensors for automotive air-bag deployment systems. The sensor portion of such an accelerometer is shown in Fig. 29.26. A central mass is suspended over the substrate, but anchored through four slender beams, which act as springs to center the mass under static-equilibrium conditions. An acceleration of the car causes the mass to deflect, reducing or increasing the clearance between the fins on the mass and the stationary fingers on the substrate.

By measuring the electrical capacitance between the mass and fins, the deflection of the mass (and therefore the acceleration or deceleration of the system) can be directly measured. Figure 29.26 shows an arrangement for the measurement of acceleration in one direction, but commercial sensors employ several masses so that accelerations can be measured in multiple directions simultaneously.

Figure 29.27 shows a 50-g surface micro-machined accelerometer (ADXL-50), with onboard signal conditioning and self-diagnostic electronics. The polysilicon sensing element (visible in the center of the die) occupies only 5% of the total die area, and the whole chip measures 500 $\mu$m $\times$ 625 $\mu$m (20 $\mu$in. $\times$ 25 $\mu$in.). The mass is approximately 0.3 $\mu$g, and the sensor has a measurement accuracy of 5% over the $\pm$50-g range.

Fabrication of the accelerometer proved to be a challenge, since it required a *complementary metal-oxide-semiconductor* (CMOS) fabrication sequence to be integrated closely with a surface micromachining approach. Analog Devices, Inc., was able to modify a CMOS production technique to directly incorporate surface micromachining. In the sensor design, the $n+$ doped silicon underpasses connect the sensor area to the electronic circuitry, replacing the usual heat-sensitive aluminum connect lines. Most of the sensor processing is inserted into the

**FIGURE 29.26**  Schematic illustration of a microacceleration sensor. *Source:* After N. Maluf.



**FIGURE 29.27** Photograph of Analog Devices' ADXL-50 accelerometer with a surface micromachined capacitive sensor (center), on-chip excitation, and self-test and signal-conditioning circuitry. The entire chip measures 0.500 mm $\times$ 0.625 mm. *Source:* After R.A. Core.

fabrication process right after a borosilicate-glass planarization process.

After the planarization, a designated sensor region, or *moat*, is cleared in the center of the die (step 1 in Fig. 29.28). A thin oxide is then deposited to passivate the $n+$ underpass connects, followed by a thin, low-pressure chemical-vapor deposited (LPCVD) nitride to act as an etch stop for the final
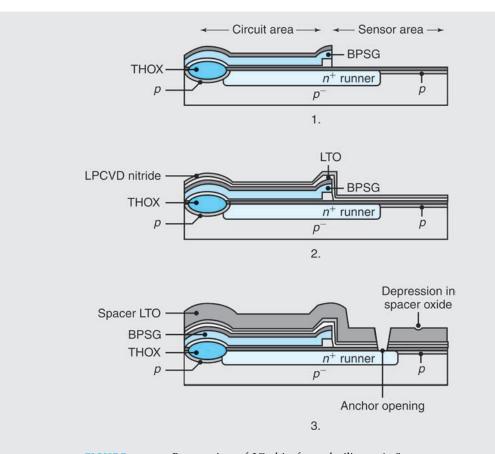
(*continued*)

**FIGURE 29.28**  Preparation of IC chip for polysilicon. 1. Sensor area post-borophosphosilicate glass (BPSG) planarization and moat mask. 2. Blanket deposition of thin oxide and thin nitride layer. 3. Bumps and anchors made in low-temperature oxide (LTO) spacer layer. *Source:* From T.A. Core, et al., *Solid State Technol.*, v. 36, pp. 39–47, 1993. Printed by permission of PennWell Corporation.

polysilicon released etching (step 2 in Fig. 29.28). The spacer or sacrificial oxide used is a 1.6-$\mu$m (64-$\mu$in.) densified low-temperature oxide (LTO), deposited over the whole die (step 3 in Fig. 29.28).

In a first etching, small depressions (that will form bumps or dimples on the underside of the polysilicon sensor) are created in the LTO layer. These bumps will limit adhesive forces and sticking in the event that the sensor comes in contact with the substrate. A subsequent etching step cuts anchors into the spacer layer, to provide regions of electrical and mechanical contact (step 3 in Fig. 29.28). The 2-$\mu$m (80-$\mu$in.) thick sensor of polysilicon layer

is deposited, implanted, annealed, and patterned (step 1 in Fig. 29.29).

Metallization follows, starting with the removal of the sacrificial spacer oxide from the circuit area, along with the LPCVD nitride and LTO layer. A low-temperature oxide is deposited on the polysilicon-sensor part, and contact openings appear in the IC part of the die, where platinum is deposited to form platinum silicide (step 2 in Fig. 29.29). The trimmable thin-film material (TiW barrier metal) and Al–Cu interconnect metal are sputtered on and patterned in the IC area.
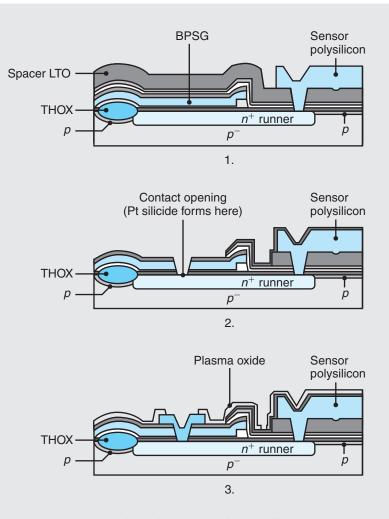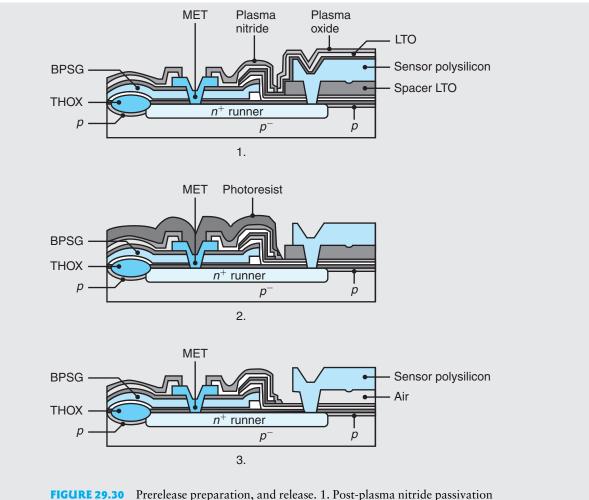
**FIGURE 29.29**  Polysilicon deposition and IC metallization. 1. Cross-sectional view after polysilicon deposition, implanting, annealing, and patterning. 2. Sensor area after removal of dielectrics from circuit area, contact mask, and platinum silicide. 3. Metallization scheme and plasma-oxide passivation and patterning. *Source:* From T.A. Core, et al., *Solid State Technol.*, v. 36, pp. 39–47, 1993. Printed by permission of PennWell Corporation.

The circuit area is then passivated in two separate deposition steps. First, plasma oxide is deposited and patterned (step 3 in Fig. 29.29), followed by a plasma nitride (step 1 in Fig. 29.30), to form a seal with the previously deposited LCVD nitride. The nitride acts as a hydrofluoric-acid barrier in the subsequent etch release in surface micromachining. The plasma oxide left on the sensor acts as an etch stop for the removal of the plasma nitride (step 1 in Fig. 29.30). The sensor area is then prepared for the final release etch. The dielectrics are removed from the sensor, and the final protective resist mask is applied. The photoresist protects the circuit area from the long-term buffered oxide etch (step 2 in Fig. 29.30). The final device cross-section is shown in step 3 in Fig. 29.30.

*Source:* Adapted from M. Madou, *Fundamentals of Microfabrication*, 2nd ed., CRC Press, 2002.

**FIGURE 29.30**   Prerelease preparation, and release. 1. Post-plasma nitride passivation and patterning. 2. Photoresist protection of the IC. 3. Freestanding, released polysilicon beam. *Source:* From T.A. Core, et al., *Solid State Technol.*, v. 36, pp. 39–47, 1993. Printed by permission of PennWell Corporation.

## 29.5   Nanoscale Manufacturing

In *nanomanufacturing*, parts are produced at nanometer length scales; the term usually refers to manufacturing below the micrometer scale, or between $10^{-9}$ and $10^{-6}$ m in length. Many of the features in integrated circuits are at this length scale, but very little else has significant relevance to manufacturing. Molecularly engineered medicines and other forms of biomanufacturing are the only commercial applications at present, except for some limited uses of carbon nanotubes (see Section 8.8). However, it has been recognized that many physical and biological processes act at this length scale; consequently, the approach holds much promise for future innovations.

Nanoscale manufacturing techniques are outlined in Table 29.3. Nanomanufacturing takes two basic approaches: top down and bottom up. **Top-down** approaches use *large building blocks* (such as a silicon wafer; see Fig. 28.2) and various manufacturing processes (such as lithography, and wet and plasma etching) to construct ever smaller features and products (microprocessors, sensors, and probes). At the other

**TABLE 29.3**

| Comparison of Nanoscale Manufacturing Techniques | | | | | |
|---|---|---|---|---|---|
| Characteristic | Top down | | | Both top down and bottom up | Bottom up | |
| Nanopatterning technique | Photo-lithography | Electron beam lithography | Nanoimprint lithography | Dip pen nanolithography | Microcontact printing | Scanning tunneling microscopy |
| Material flexibility | No | No | No | Yes | Yes | Limited |
| Resolution | ~35 nm | ~15 nm | ~10 nm | 14 nm | ~100 nm | Atomic |
| Registration accuracy | High | High | High | Extremely high | Low | Extremely high |
| Speed | Very fast | Moderate | Fast | Slower, but scalable | Fast | Very slow |
| Cycle time | Weeks | Days | Days–week | Hours | Days–weeks | Days |
| Cost | | | | | | |
|   Purchase | >$10 M | >$1 M | >$500K | <$250 K | ~$200 K | >$250 K |
|   Operation | High | High | Moderate | Low | Moderate | Low |

*Source:* Courtesy of NanoInk, Inc. Reprinted by permission.

extreme, **bottom-up** approaches use *small building blocks* (such as atoms, molecules, or clusters of atoms and molecules) to build up a structure. In theory, bottom-up approaches are similar to the additive manufacturing technologies described in Section 20.3. When placed in the context of nanomanufacturing, however, bottom-up approaches suggest the manipulation and construction of products are on an atomic or molecular scale.
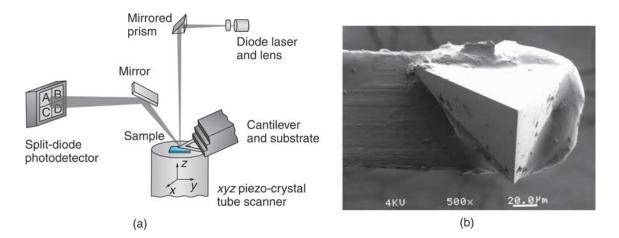
Bottom-up approaches are widely used in nature (e.g., building cells is a fundamentally bottom-up approach), whereas conventional manufacturing has, for the most part, consisted of top-down approaches. In fact, there are presently no nanomanufactured products (excluding medicines and drugs "manufactured" by bacteria) that have demonstrated commercial viability.

Bottom-up approaches in various research applications can use atomic-force microscopy (AFM) for the manipulation of materials on the nanoscale. Figure 29.29 is an illustration of an atomic-force microscope. A probe (Fig. 29.31b) is mounted into the microscope, and a laser is reflected from a mirror on the back side of the probe so that it reflects onto a set of photosensors. Any vertical or torsional deflection of the cantilever is registered as a change in voltage on the photosensors. Atomic-force microscopes can have true atomic resolution of $<1 \times 10^{-10}$ m.
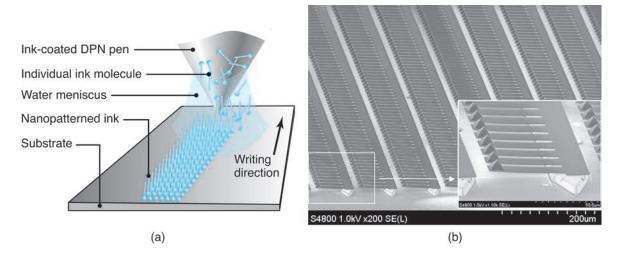
Atomic-force microscopes are widely used to measure the surface profile of very smooth surfaces (Section 33.3). Several approaches have been developed to allow nanoscale manufacturing processes to be performed on these microscopes. Some top-down approaches are:

- **Photolithography, electron-beam lithography, and nanoimprint (soft) lithography**.  These techniques are capable of top-down manufacture of structures, with resolution under 100 nm, as discussed in Section 28.7.
- **Nanolithography.**  The probes used in atomic-force microscopy vary greatly in size, materials, and capabilities. The diamond-tipped stainless-steel cantilever shown in Fig. 29.31b has a tip radius of around 10 nm. By contacting and plowing across a surface, it can produce grooves up to a few $\mu$m thick. The spacing between lines depends on the groove depth needed.

- **Dip pen nanolithography.** This approach (Fig. 29.32) is used in an atomic-force microscope to transfer chemicals onto substrates. The process can produce lines as narrow as 10 nm. Dip pen nanolithography can be used with many parallel pens (Fig. 29.32b), typically made of silicon nitride and containing as many as 55,000 pens in a 1-cm$^2$ area. In a top-down approach, dip pen nanolithography is used to produce a mask suitable for lithography.



(a)

(b)

**FIGURE 29.31**   (a) Schematic illustration of an atomic-force microscope. A probe is mounted on a cylinder containing piezoelectric material; this arrangement allows translation of the probe in three dimensions. A laser, reflected from a mirror on the back of the probe onto a set of photosensors, allows measurement of the probe's location and monitoring of interactions with a sample surface. (b) Scanning-electron microscope image of a diamond-tipped stainless-steel cantilever suitable for nanolithography.



(a)

(b)

**FIGURE 29.32**   (a) Schematic illustration of dip pen nanolithography. (b) An array of pens used to produce identical patterns on surfaces. Commercial pen arrays can contain up to 55,000 pens; only a fraction of the available pens are shown. The inset highlights individual cantilevers, showing the 7.5-$\mu$m-high tips. *Source:* Courtesy of NanoInk, Inc.

Bottom-up approaches include:

- Dip pen nanolithography also can be a bottom-up approach, wherein the ink contains the material used to build the structure.
- *Microcontact printing* uses soft-lithography approaches, to deposit material on surfaces from which nanoscale structures can be produced.
- *Scanning tunneling microscopy* can be used to manipulate an atom on an atomically smooth surface (usually cleaved mica or quartz).

## SUMMARY

- MEMS is relatively new and developing rapidly. Although most successful commercial MEMS applications are in the optics, printing, and sensor industries, the possibilities for new device concepts and circuit designs appear to be endless.
- MEMS devices are manufactured through techniques and with materials that, for the most part, have been pioneered in the microelectronics industry. Bulk and surface micromachining are processes that are well developed for single-crystal silicon.
- Specialized processes for MEMS include variations of machining, such as DRIE, SIMPLE, and SCREAM. These processes produce freestanding mechanical structures in silicon.
- Polymer MEMS can be manufactured through LIGA or microstereolithography. LIGA combines X-ray lithography and electroforming to produce three-dimensional structures. Related processes include multilayer X-ray lithography and HEXSIL.
- Nanoscale manufacturing is a relatively new area that has significant potential. The processes are typically bottom up, whereas conventional manufacturing is top down. Some lithography processes extend to the nanoscale, as does dip pen lithography. Materials such as carbon nanotubes have great potential for nanoscale devices.

## KEY TERMS

| | | | |
|---|---|---|---|
| Atomic-force microscope | HEXSIL | Multilayer X-ray | SIMPLE |
| Bulk micromachining | LIGA | lithography | Stiction |
| Diffusion bonding | MEMS | Planarization | Surface |
| Dip pen nanolithography | Micromachining | Sacrificial layer | micromachining |
| EFAB | Microstereolithography | SCREAM | UV-LIGA |
| Electrochemical fabrication | MolTun | Silicon-LIGA | |

## BIBLIOGRAPHY

Adams, T.M., and Layton, R.W., **Introductory MEMS: Fabrication and Applications**, Springer, 2009.

Allen, J.J., **Microelectromechanical System Design**, CRC Press, 2006.

Elwenspoek, M., and Jansen, H., **Silicon Micromachining**, 2nd ed., Cambridge University Press, 2004.

Elwenspoek, M., and Wiegerink, R., **Mechanical Microsensors**, Springer, 2001.

Fraden, J., **Handbook of Modern Sensors: Physics, Designs, and Applications,** 4th ed., Springer, 2010.

Gad-el-Hak, M. (ed.), **The MEMS Handbook**, 2nd ed. (3 vols.), CRC Press, 2006.

Ghodssi, R., and Lin, P. (eds.), **MEMS Materials and Processes Handbook**, Springer, 2011.

Harper, C.A. (ed.), **Electronic Packaging and Interconnection Handbook**, 4th ed., McGraw-Hill, 2004.

Hsu, T.-R., **MEMS & Microsystems: Design, Manufacture, and Nanoscale Engineering**, 2nd ed., Wiley, 2008.

Jha, A.R., **MEMS and Nanotechnology-based Sensors and Devices for Communications, Medical and Aerospace Applications**, CRC Press, 2008.

Kempe, V., **Inertial MEMS: Principles and Practice**, Cambridge, 2011.

Korvink, J., and Oliver, P. (eds.), **MEMS: A Practical Guide to Design, Analysis, and Applications**, William Andrew, 2005.

Leondes, C.T., **MEMS/NEMS Handbook** (5 vols.), Springer, 2007.

Liu, C., **Foundations of MEMS**, 2nd ed., Prentice Hall, 2011.

Madou, M.J., **Manufacturing Techniques for Microfabrication and Nanotechnology**, CRC Press, 2009.

Madou, M.J., **Applications of Microfabrication and Nanotechnology**, CRC Press, 2009.

Maluf, N., **An Introduction to Microelectromechanical Systems Engineering**, 2nd ed., Artech House, 2004.

Nishi, Y., and Doering, R. (eds.), **Handbook of Semiconductor Manufacturing Technologies**, 2nd ed., CRC Press, 2007.

Rockett, A., **The Materials Science of Semiconductors**, Springer, 2008.

Schaeffer, R., **Fundamentals of Laser Micromachining**, Taylor & Francis, 2012.

Sze, S.M., **Semiconductor Devices: Physics and Technology**, 3rd ed., Wiley, 2012.

Varadan, V.K., Jiang, X., and Varadan, V., **Microstereolithography and Other Fabrication Techniques for 3D MEMS**, Wiley, 2001.

## REVIEW QUESTIONS

**29.1** Define MEMS, SIMPLE, SCREAM, and HEXSIL.

**29.2** Give three examples of common microelectromechanical systems.

**29.3** Why is silicon often used with MEMS devices?

**29.4** Describe bulk and surface micromachining.

**29.5** What is the purpose of a spacer layer in surface micromachining?

**29.6** What is the main limitation to successful application of MEMS?

**29.7** What are common applications for MEMS and MEMS devices?

**29.8** What is LIGA? What are its advantages?

**29.9** What is a sacrificial layer?

**29.10** Explain the differences between stereolithography and microstereolithography.

**29.11** What is MolTun? What are its main advantages?

**29.12** What is HEXSIL?

**29.13** What do SIMPLE and SCREAM stand for?

## QUALITATIVE PROBLEMS

**29.14** Describe the difference between isotropic etching and anisotropic etching.

**29.15** Lithography produces projected shapes, so true three-dimensional shapes are more difficult to produce. What lithography processes are best able to produce three-dimensional shapes, such as lenses? Explain.

**29.16** Which process or processes in this chapter allow the fabrication of products from polymers?

**29.17** What is the difference between chemically reactive ion etching and dry-plasma etching?

**29.18** The MEMS devices discussed in this chapter are applicable to macroscale machine elements, such as spur gears, hinges, and beams. Which of the following machine elements can or cannot be applied to MEMS, and why? (a) Ball bearings, (b) bevel gears, (c) worm gears, (d) cams, (e) helical springs, (f) rivets, and (g) bolts.

**29.19** Explain how you would produce a spur gear if its thickness was one-tenth of its diameter and its diameter was (a) 1 mm, (b) 10 mm, and (c) 100 mm.

**29.20** List the advantages and disadvantages of surface micromachining compared with bulk micromachining.

**29.21** What are the main limitations to the LIGA process? Explain.

**29.22** Other than HEXSIL, what process can be used to make the microtweezers shown in Fig. 29.23? Explain.

**29.23** Is there an advantage to using the MolTun process for other materials? Explain.

## QUANTITATIVE PROBLEMS

**29.24** The atomic-force microscope probe shown in Fig. 29.31 has a stainless steel cantilever that is 450 $\mu$m × 40 $\mu$m × 2 $\mu$m. Using equations from solid mechanics, estimate the stiffness of the cantilever, and the force required to deflect the end of the cantilever by 1 $\mu$m.

**29.25** Estimate the natural frequency of the cantilever in Problem 29.24. *Hint:* See Problem 3.21.

**29.26** Tapping-mode probes for the atomic-force microscope are produced from etched silicon and have typical dimensions of 125 $\mu$m in length, 30 $\mu$m in width, and 3 $\mu$m in thickness. Estimate the stiffness and natural frequency of such probes.

**29.27** Using data from Chapter 28, derive the time needed to etch the hinge shown in Fig. 29.7 as a function of the hinge thickness.

**29.28** It is desired to produce a 500 $\mu$m by 500 $\mu$m diaphragm, 25 $\mu$m thick, in a silicon wafer 250 $\mu$m thick.

Given that you will use a wet etching technique, with KOH in water with an etch rate of 1 $\mu$m/min, calculate the etching time and the dimensions of the mask opening that you would use on a (100) silicon wafer.

**29.29** If the Reynolds number for water flow through a pipe is 2000, calculate the water velocity if the pipe diameter is (a) 10 mm; (b) 100 $\mu$m. Do you expect flow in MEMS devices to be turbulent or laminar? Explain.

# SYNTHESIS, DESIGN, AND PROJECTS

**29.30** List similarities and differences between IC technologies described in Chapter 28 and miniaturization technologies presented in this chapter.

**29.31** Figure I.7b in the General Introduction shows a mirror that is suspended on a torsional beam, and can be inclined through electrostatic attraction by applying a voltage on either side of the micromirror at the bottom of the trench. Make a flowchart of the manufacturing operations required to produce this device.

**29.32** Referring to Fig. 29.5, design an experiment to find the critical dimensions of an overhanging cantilever that will not stick to the substrate.

**29.33** Design an accelerometer by using (a) the SCREAM process and (b) the HEXSIL process.

**29.34** Design a micromachine or device that allows the direct measurement of the mechanical properties of a thin film.

**29.35** Conduct a literature search and determine the smallest diameter hole that can be produced by (a) drilling, (b) punching, (c) water-jet cutting, (d) laser machining, (e) chemical etching, and (f) EDM.

**29.36** Perform a literature search and write a one-page summary of applications in biomes.